



Humidification Effect on the Performance and Emissions of (DI) Diesel Engine Running on Diesel Fuel with Biodiesel Blended Nano Additives

Hussein Jumaa^{a*}, Mahmoud A. Mashkour^b

^a MSc Student, Mechanical Engineering Department, University of Technology, Baghdad, Iraq
hussainjumaa92@gmail.com

^b Mechanical Engineering Department, University of Technology, Baghdad, Iraq
20087@uotechnology.edu.iq

* Corresponding author.

Submitted: 23/11/2020

Accepted: 14/03/2021

Published: 25/05/2021

KEYWORDS

Diesel Engine,
Performance, Emissions,
Air Humidification,
Waste cooking oil, Iron
oxide Nanoparticle,
Taguchi method.

ABSTRACT

The effect of humidification of the air on the performance of a compression ignition engine operating on diesel, biodiesel with nano additives was investigated. The experiment was carried out on a single-cylinder, four-stroke, naturally aspirated water-cooled, direct injection Ricardo (E6/US) diesel engine at a constant speed of 1800 rpm, and varying loads. A mixture of Biodiesel (waste cooking oil) and diesel fuel by four ratios (B5, B10, B15, and B20) was used in the experiment. Besides, five concentrations of Iron oxide nanoparticles (Fe₂O₃, with particle size 20 nm) as fuel-additives were prepared (10 ppm, 30 ppm, 50 ppm, 70 ppm, and 100 ppm), and added to the test fuels (Bio-Diesel). Taguchi Method by DOE was used for the optimization in this investigation. The results of Taguchi Method experiments identified the biodiesel (B20), nano additive (100 ppm), relative humidity (65%). The experimental results manifested that BTE improved by 17.62% and BSFC decreased by 12.72%, while NO_x and PM reduced by 8.45%, 24.17%, respectively.

How to cite this article: M. A. Mashkour and H. J. Jamil, "Humidification Effect on the Performance and Emissions of (DI) Diesel Engine Running on Diesel Fuel with Biodiesel Blended Nano Additives", Engineering and Technology Journal, Vol. 39, Part A, No. 05, pp. 790-803, 2021

DOI: <https://doi.org/10.30684/etj.v39i5A.1935>

This is an open access article under the CC BY 4.0 license <http://creativecommons.org/licenses/by/4.0>

1. INTRODUCTION

The mindfulness of energy concerns and environmental glitches correlated to the burning of petroleum-based fuels has fortified numerous researchers to examine the opportunity of utilizing non-conventional energy sources, as an alternate fuel source to fossil fuels and their derivatives [1,2]. It has enhanced a global agenda to improve clean substitute fuels that are readily available, globally acceptable, and technically feasible. Renewable energy sources have a very high potential and enormous availability, making them meet numerous times the earth's energy demand. Biodiesel has emerged as the most popular alternative fuel source for diesel [3].

The application of biodiesel in C. I. engine has some limitations, such as an increase in fuel consumption, lower calorific value, higher density, lower cloud and pour points, high NO_x emission, and cold starting problems [4-6]. These disadvantages can be overcome by using nano additives, and it results in an enhancement in the physicochemical properties, such as the density, calorific value, viscosity, cetane number with improvement in combustion characteristics, shorter ignition delay, and cold starting problems [7-9]. Water addition is employed to restrict NO_x emissions sourced from diesel engines. Atomized water droplets enable a significant decrease in combustion temperature during combustion which results in a lower level of NO_x and improves the atomization characteristics of injected fuel [10]. B. V. Appa Rao, et al. [11] investigated the performance and exhaust emissions using Mahua Methyl Ester (biodiesel) with water fumigation at the suction end of a diesel engine, a single-cylinder, four-stroke, 5 hp, constant speed 1500 rpm, direct injection type vertical and 16.5 compression ratio. The superheated water vapor in mass quantities of (0.25, 0.5, and 0.75 kg/hr) has been sent to the suction of the engine along with the aspirated air, and the mass flow of the water into the evaporator was controlled by a rotameter designed to achieve the required mass flow rates. It was found that the brake thermal efficiency was highest for 0.25 kg/hr water vapor at the suction, and the specific fuel consumption for the various percentages of water fumigation was observed to be in between diesel and pure biodiesel at all loads. NO_x emission was found to be reduced at all percentages of the water fumigation, while the CO and HC emissions increased when compared to the diesel fuel at all loads. B. T. R. Mishra, et al. [12] experimentally studied the combustion, performance, and emission characteristics of a compression ignition engine running with biodiesel under steady-state conditions with a novel NO_x reducing mechanism involving a water injections system. The experimental work was conducted on a four-cylinder, four strokes, direct injection (DI) turbocharged diesel engine. Biodiesel produced from the rapeseed oil by transesterification process was used. The experimental results showed that the water injection at a rate of 3 kg/h produced a reduction in NO_x emission by about 50% without causing any significant change in the specific fuel consumption. M. Y. E. Selim, et al. [13] investigated the effect of the water-waste cooking oil (WCO) biodiesel emulsion on performance, engine roughness, and exhaust emissions of a single-cylinder four-stroke diesel engine, naturally aspirated, with variable injection timing and compression ratio. Biodiesel blended with a percentage was (5%, 10%, and 15%), where the tested was under different engine speeds and loads. Results depicted that the engine produced slightly less output torque when the WCO biofuel and emulsions with water were used, hence, the brake fuel consumption slightly increased. Furthermore, the water in biofuel emulsion is used to reduce the dangerous emissions of NO_x. A. Parlak, et al. [14,15] investigated the effects of performance and emissions using a steam injection of a single-cylinder diesel engine, naturally aspirated, four-stroke, water-cooled direct injection fueled with tobacco seed oil methyl ester (TSOME) and canola oil methyl ester (COME) blends. Biodiesel fuel was blended with diesel fuel (B10, B20) vol%. The steam ratio with a percentage of 10% was found as optimum for exhaust emissions, both NO_x and smoke emissions decreased. R. Singh, et al. [16] checked the effect of titanium oxide nanoparticle blended water-diesel emulsion on the performance and emission characteristics of a single-cylinder, four-stroke diesel, engine water-cooled VCR engine with constant speed (1500 rpm) and various loads. Water addition was (10%) and (15%), and the addition of titanium oxide (TiO₂) nanoparticle was (50 ppm) and (70 ppm). It was concluded that the titanium oxide nanoparticle blended water-diesel emulsion does not only enhance the performance characteristics but also helps in the reduction of harmful emissions HC and CO. H. Bandbafhaa, et al. [17] studied the impact of water addition by (3% l/sec) and aqueous carbon nanoparticles (38 ppm, 75 ppm, and 150 ppm) in water-emulsified diesel-biodiesel blends on the performance and emissions parameters of a diesel engine at a fixed engine speed of (1000 rev/min) under four different engine loads ranging from (25%) to (100%) of full load conditions. The result showed that the emulsified fuel blend containing (38 ppm) carbon nanoparticles increased the brake power and the brake thermal efficiency by 1.07 kW and 11.58% at full load operation, respectively, while it led to the decreased brake specific fuel consumption by 107.3 g/kW. h, and adversely affected HC and CO at full load conditions owing to an increase in the carbon content of the fuel blends but it lowered NO_x. M. Abdollahia, et al. [18] checked the effects of nano-emulsion biodiesel fuel on the engine efficiency, emission parameters, and combustion characteristic of 12 hp Lombardini single cylinder air cooled diesel engine. Nano-emulsion fuel was produced from 5% waste cooking oil biodiesel and 5% distilled water using ultrasonic waves for stabilizing 5 vol% (tween 80 and spans 80) surfactants in HLB8 (Hydrophilic-Lipophilic Balance). The results evinced that the diesel engine power and torque using nano-emulsion fuel improved by about 4.84% and 4.65%, respectively, and significantly

reduced the CO, HC, NO_x, and Soot opacity by 11%, 6%, 9%, and 10%, respectively, and CO₂ small rise by 7%, compared to diesel fuel.

This work objectives to study the impact of changing the humidity of air on engine performance and emissions of fueled diesel, biodiesel 'Waste Methyl Ester (WME)' blended, and nanoparticle of iron oxide (Fe₂O₃). Taguchi method of experimental design is used to selecting the optimal performance parameters for testing on the diesel engine.

2. EXPERIMENTAL STUDY:

I. Experimental Setup and Measurement

This study was carried out at the Internal Combustion Engines Laboratory at the University of Technology. A single-cylinder four-strokes research diesel engine of type (Ricardo E6/US) was used in this study. The details of the engine specifications used in the investigation in Table I. The engine is mated to a DC dynamometer so that the engine speed and power can be set independently. The exhaust gas temperature was measured by using a thermocouple (K-type) and a GEMO-DT109A digital reader. EA-CG450 analyzer was utilized to measure the exhaust emissions constituents, such as CO, HC, NO_x, CO₂, O₂. Each smoke opacity and particulate matter was measured using AVL-491 opacimeter and Aerocet-531, respectively. The test rig was set up as shown in Figures 1, 2 where represent the schematic layout of the test setup and the test engine, respectively, and a photographic picture of the engine and its accessories.

TABLE I: Tested engine specifications

Engine model	Ricardo E6/US
Engine type	Single cylinder, Four stroke, Direct injection diesel engine
Swept volume	507 cc
Bore	76.2 mm
Stroke	111.1 mm
Compression ratio	4.5-22 (variable)
Rated brake power	9 kW, Natural aspirated
Rated speed	1800 rpm
Cooling system	Water cooled
Nozzle opening pressure	150 bar
Injection timing	(20-45 °) (variable)

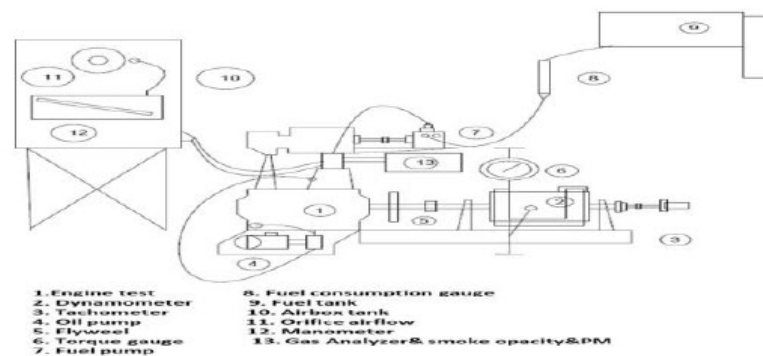


Figure 1: Schematic diagram of test engine setup.



Figure 2: Ricardo engine and its accessories.

II. Biodiesel preparation

Waste cooking oil obtained from the restaurants is considered as feedstock for biodiesel production. The transesterification process is a chemical method of converting large, branched, triglyceride molecules of waste cooking oils and fats into smaller, straight-chain molecules, almost identical in size to the molecules of the species found in diesel fuel. The process takes place by reacting in the presence of a catalyst with alcohol in the vegetable oil. The waste cooking oil was preheated to 75°C to dilute it and get rid of the humidity. Potassium methoxide was prepared from 25% (v / v oil) of methanol (6:1 molar ratio) and 1.5% (m / m oil) of potassium hydroxide (KOH) by dissolving the potassium hydroxide in the methanol. Where, the reaction was held at 60°C in the mixing machine to achieve yield for the optimized potassium hydroxide (KOH) concentration and the methanol alcohol proportion. The methoxide was mixed with preheated waste oil and the reaction was carried out for (two hours) by stirring with a mechanized stirrer at nominal speed and a steady reaction temperature of 55°C. The chemical reaction takes place during the period between the raw of (WCO) and methanol. At the end of reaction completion, the mixture was drained and transferred to the separating funnel. In the funnel, the separation phase was found in two layers. The upper layer was biodiesel and the lower phase was glycerin. Finally, to eliminate the excess alcohol, methyl ester was washed several times with distilled water and then heated to 110°C. The sodium sulfate (Na_2SO_4) was used for dry of the product. Finally, to filter the substance, a qualitative filter paper was used. The final product was very yellow. The process of biodiesel production is presented in Figure 3. Biodiesel was mixed with diesel oil at different proportions of (B5, B10, B15, and B20) vol.%.



Figure 3: Process of biodiesel production.

III. Nanoparticle additive

Nanoparticles are a nano powder added to the fuel to improve the physical properties, such as viscosity, density, cetane number, flash point, and calorific value, also, improves the thermal properties of the fuel. The used nanoparticle is an Iron oxide nanoparticle (Fe_2O_3) produced by Nanjing Nano Technology-China, purity 99%, particle size (20-30) nm, and it was received from a special agent for chemicals in Baghdad. Then, it was tested in Alsa lam Nanotechnology and the Advanced Materials Research Center at the University of Technology-Baghdad/ Iraq, as shown in Figure 4. The specifications of the used nano powder Fe_2O_3 are given in Table II.

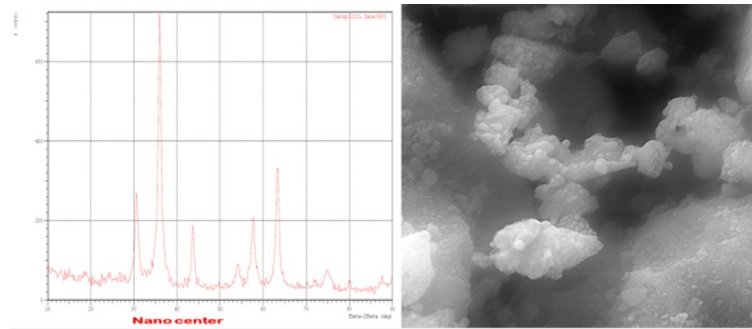


Figure 4: XRD and SEM images of nanoparticles Fe_2O_3 .

TABLE II: The specification of nanoparticles- Fe_2O_3

Item	Nano- Fe_2O_3 specifications
Manufacturer	Nanjing Nano. Alpha-China
Appearance	Red brown powder
Assay	99%
Structure	Spherical
Crystal and type	$\alpha\text{-Fe}_2\text{O}_3$
Particle size nm	20–30 nm
pH value	5-7
Specific Surface area (m^2/g)	40-60
Bulk density	1.20 g/cm^3
True density	g/cm^3
Thermal conductivity	7 W/m.K

IV. Preparation of nano-fuel

The diesel fuel (gas oil) was obtained from the Dura-Refinery in Baghdad-Iraq, and the biodiesel was prepared from waste cooking oil by transesterification process. The Iron oxide nanoparticle (Fe_2O_3) was obtained from a local supplier in Baghdad. Nano fuel was prepared by mixing biodiesel blended with nanoparticle iron oxide (Fe_2O_3) with different percentages (10 ppm, 30 ppm, 50 ppm, 70 ppm, and 100 ppm) wt%. Nanoparticles have a higher surface area, surface power great, and they appear to agglomerate and begin to sediment to form a micro molecule. So, the ultrasonicated device was used to prevent this drawback. The mixing process takes place in an ultrasonic device for two hours for one sample to obtain homogeneous nano fuel. The preparation processes and the physical properties of diesel fuel, blended biodiesel with nano additives are shown in Figure 5 and Table III.



Figure 5: Nano fuel prepared method.

TABLE III: Physical characteristics of diesel, biodiesel,nano-fuel

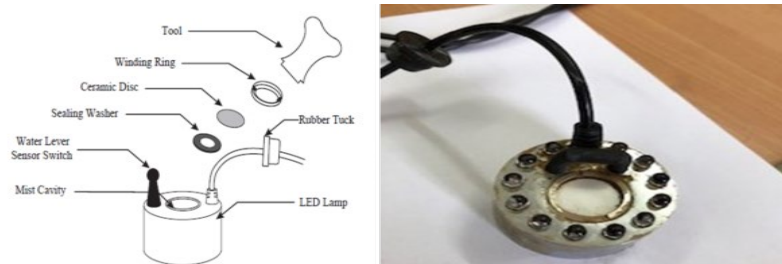
Fuel Sample	Diesel (vol%)	Biodiesel (vol%)	n-Fe ₂ O ₃ (wt%)	K.V (cSt)	Density (kg/m ³)	CN	LCV (kJ/kg)	Flashpoint (°C)	Firepoint (°C)
Diesel	100	-----	-----	2.72	840	53	42,500	67	86
B20	80	20	-----	3.3	847.1	53.4	41,400	71.5	92
B20+ 10 ppm	80	20	10ppm	3.30	847.9	53.5	41,414	72.1	92.6
B20+30 ppm	80	20	30ppm	3.31	849.64	53.6	41,521	72.4	92.9
B20+50 ppm	80	20	50ppm	3.316	851.33	53.7	41,607	72.7	93.1
B20+70 ppm	80	20	70ppm	3.32	853.02	53.8	41,690	73.2	93.6
B20+100 ppm	80	20	100ppm	3.35	860.57	53.9	41,814	73.5	94

V. Air Humidification (Ultrasonic Mist Maker)

An ultrasonic mist generator consists of a compact mist maker provided with a single head ultrasonic transducer, immersed in a tank with a level of steady water, where the water atomization process is properly controlled. The ultrasonic transducer composes of a piezoelectric crystal coupled to a 16-mm diameter ceramic disc, as shown in Table IV the unit's technical specifications. When submerged in the water, the transducer is capable of transforming high-frequency electronic signals, typically ranging from 0.8 to 1.7 MHz into high-frequency mechanical oscillations on the disc. When the water attempts to follow the movements of the ceramic disc, it is unable to keep up with the high-frequency oscillations. As a result, on the negative oscillations, the water is detached from the disc and produces a transitory vacuum where the water cavitates and changes into steam. Then on the positive oscillation, the high-pressure wave drives the steam water through the water surface. A fine water mist is formed in this adiabatic process, with droplet diameters on the scale of a few tens of microns, which are readily incorporated into the airflow [19], as shown in Figure 6.

TABLE IV: Ultrasonic mist maker specifications

Ceramic disc plated material	Nickel or Titanium
Generate mist (ml/h)	> 450 ml/h
Ceramic core diameter	16 mm
Working Voltage AC	24 V
Working Electric current (ma)	500 mA
Ultrasonic Frequency(kHz)	1700 ± 40 kHz
Working water temperature	0 – 45 °C
Working water level	25 – 45 mm
Lifespan of Ceramic disc (hour)	> 3000

**Figure 6: Parameter ultrasonic mist maker.**

The ultrasonic mist maker is used to generate fumes in the airbox to change the humidity of the air entering the engine. The device operation steps are as follows, set the ultrasonic mist maker into a

water container and install it inside the airbox. Fill the water container by using a small pump at (3 l/min), height (0.4-1.5 m), and power supply 3 Watt, then Place the humidity sensor near the airbox orifice, and the other in the airway to the engine which humidity was controlled by a humidity controller type ZL-7816A. Put the transformer outside the airbox in a drafty far away

moist and plug the connector of the mist maker into the socket of the transformer properly and screw the tarpaulin tightly. Then, plug the transformer into the power supply, it will start to work immediately. The stages of installing an ultrasonic mist maker device in the intake airbox with the connection of electricity and water are shown in Figure 7.

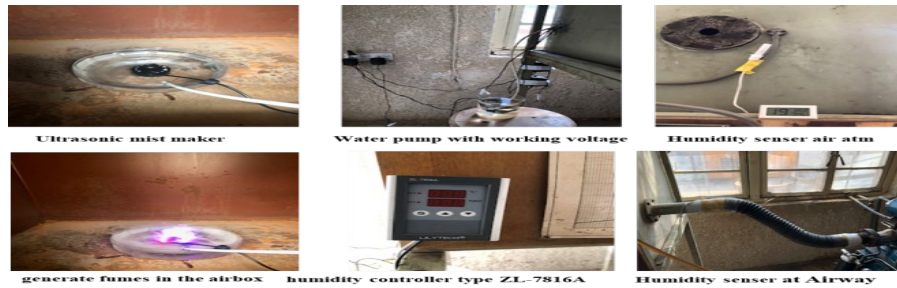


Figure 7: Steps of installing the ultrasonic mist maker device in the intake airbox.

VI. Taguchi Method of Optimization (DOE)

Taguchi method is an aggregation of numerical and statistical tools helpful for the parametric optimization and abstract thought of problems in which a response of interest is affected by various factors, and the objective is to optimize this response. Taguchi method is utilized to find out the relationship between a response and a set of quantitative experimental variables [20].

This work utilizes four variables at four levels and so, the orthogonal array (L16) was taken for the building of a practical setup. It has parameters, such as engine load, biodiesel blend, nano additives, and relative humidity, settled in a row (1, 2, 3, 4), as shown in Table V. As per this design, sixteen (16) experiments were conducted and trials were taken at random, for neglecting the systematic error creeping into the trials. The performance was evaluated and utilizing as a response variable. The better S/N ratio is utilized in this practical study as shown in Figures 8, and 9. Results obtained by analyzing performance are shown in Table VI.

TABLE V: Parameters and levels of tested fuels and humidity percentage

Factors	Level 1	Level 2	Level 3	Level 4
load (N .m)	6.855	9.14	12.34	16.45
blend (B%)	5	10	15	20
Nano (ppm)	30	50	70	100
(RH%)	20	40	55	65

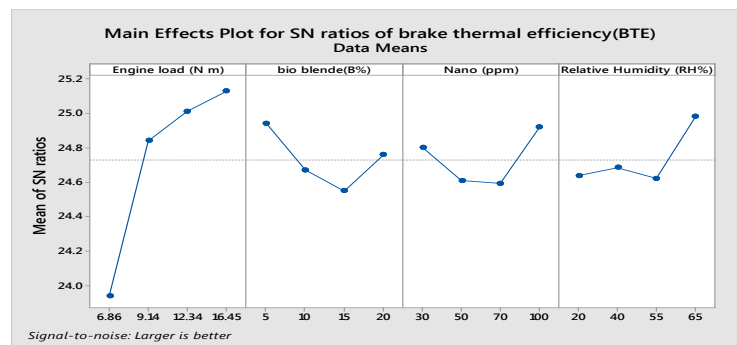


Figure 8: Response diagram of S/N ratio for BTE.

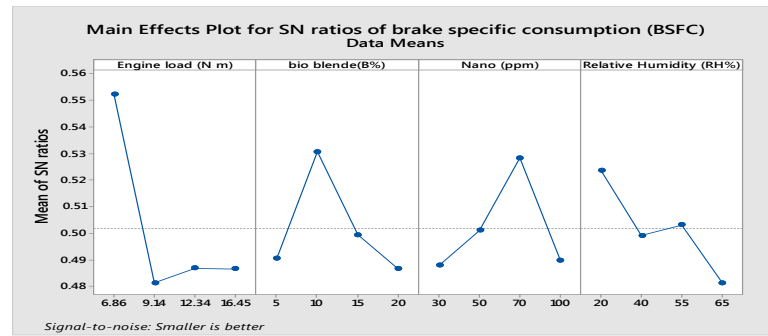


Figure 9: Response diagram of S/N ratio for BSFC.

TABLE VI: Optimum parameter settings for engine performance.

Load N.m	Biodiesel Blend (B)	Nano Additive (ppm)	RH%
16.56	B20	100	65%

3. RESULTS AND DISCUSSION

The experimental procedure involves the influence of humidification of the air on performance and emissions characteristics of a compression ignition engine operating on diesel, biodiesel with nano additives. An ultrasonic mist maker was installed inside the air intake box for changing the air humidity entering the engine. The humidity ratios used in the experiments were (20%, 40% 55%, and 65%), and the loads used in the experiments were (3.2 N. m, 6.86 N. m, 9.14 N. m, 12.34 N. m, 16.45 N. m, and 20.56 N. m). The engine speed of (1800 rpm), injection timing at (38° bTDC), and compression ratio at (17:1) were utilized. Humidity relative, nano additive ratio, and blend biodiesel were chosen according to the Taguchi method used for the optimization. The results were recorded under steady-state conditions. All the results of performance characteristics and emissions were plotted against the brake power (BP).

I. Performance characteristics:

1) Brake Thermal Efficiency (BTE)

Figure 10 reveals the variation of the brake thermal efficiency (BTE) with the brake power (BP) for all tested fuels (D100, D80:B20, and D80:B20:N100 ppm) with air humidity (RH65%). The brake thermal efficiency increased by 12.75% at the use of fuel (D80:B20), due to the presence of oxygen in biodiesel that leads to improve the combustion process and increases the rate of heat release. Also, the brake thermal efficiency increased by 15.05% with the addition of nano-Fe₂O₃ at a concentration (100 ppm) wt% for fuel (D80:B20), compared to diesel fuel, this is due to the improvement of the cetane number and calorific value of fuels. The brake thermal efficiency for fuel (D80:20:N100 ppm) increased with changing air humidity of the intake into the engine of (RH65%) by 17.63%, compared to pure diesel, due to that the increased humidity of the air into the intake of combustion chamber leads to a delay in the ignition period, as the longer the ignition period leads to the formation of a homogeneous air-fuel mixture increasing the rate of heat release [17,18].

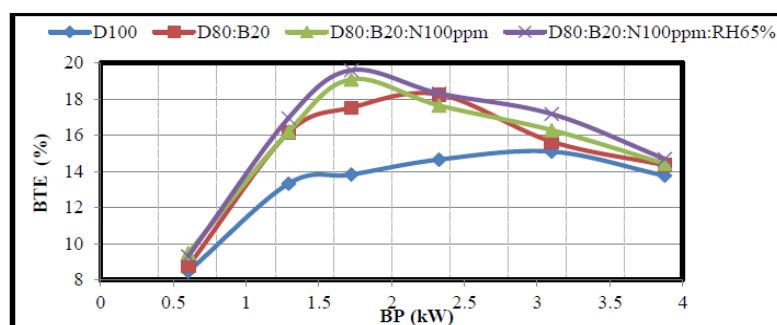


Figure 10: Variation in BTE with BP.

2) Brake Specific Fuel Consumption (BSFC)

Figure 11 manifests the variation of the brake specific fuel consumption (BSFC) with the brake power (BP) for all tested fuels (D100, D80:B20, and D80:B20:N100 ppm) with air humidity (RH65%). The brake fuel consumption decreased by 7.84% at the use of fuel (D80:B20), due to the higher cetane number which increased the combustion temperature. Also, the (BSFC) decreased by 11.03% by the addition of nano-Fe₂O₃ with concentration (100 ppm) wt% for fuel (D80:B20), compared to diesel fuel, this is due to catalytic chemical oxidation of fuel which in turn improves the combustion of fuel. The brake fuel consumption decreased by 15.19% for fuel (D80:20:N100 ppm) with changing the air humidity of the intake into the engine by (RH65%), compared to pure diesel. This is because of increased humidity of the air into intake of the combustion chamber, where the micro explosion produced by the water in the fuel atomized the injected fuel completely during the combustion [17].

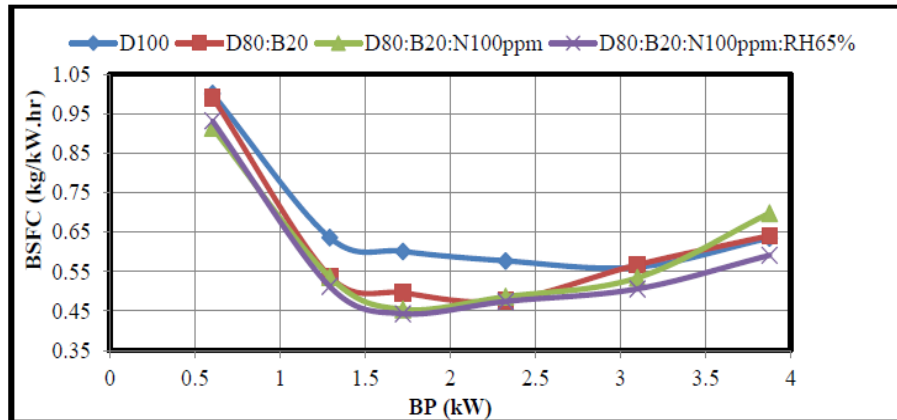


Figure 11: Variation in BSFC with BP.

3) Exhaust Gas Temperature (EGT)

Figure 12 elucidates the variation of the exhaust gas temperature (EGT) with the brake power (BP) for all tested fuels (D100, D80:B20, and D80:B20:N100 ppm) with air humidity (RH65%). The exhaust gas temperature increased by 0.5% at the use of fuel (D80:B20), due to the higher cylinder temperature caused by the completed burning of fuel. Also, the (EGT) increased by 1.7% at the addition of nano-Fe₂O₃ with concentration (100 ppm) wt% for fuel (D80:B20), compared to diesel fuel, this is due to the increased physical properties, such as cetane number for fuel which increase the cylinder temperature. But, the exhaust gas temperature decreased by 2.46% at the use of fuel (D80:20:N100 ppm) with changing the air humidity of intake into the engine of (RH65%), compared to pure diesel. This is due to the increased humidity of air into the intake combustion chamber where the evaporation of water in small liquid droplets may absorb the heat which decreases the exhaust gas temperature.

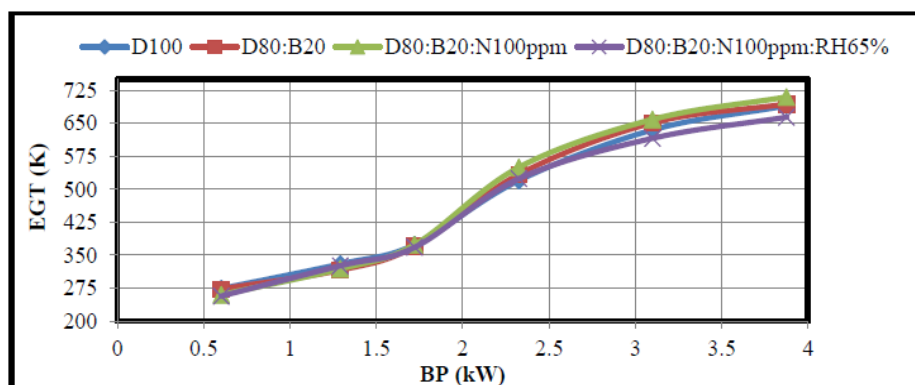


Figure 12: Variation in EGT with BP.

II. Emissions Characteristics:

1) Carbon Monoxide Emission (CO)

Figure 13 demonstrates the variation of carbon monoxide (CO) with the brake power (BP) for all tested fuels (D100, D80:B20, and D80:B20:N100 ppm) with air humidity (RH65%). Carbon monoxide decreased by 18.18% at the use of fuel (D80:B20), compared to pure diesel, due to the biodiesel content of oxygen atoms which leads to better mixing air and fuel. Then, the (CO) also decreased by 52.94% at the addition of nano-Fe₂O₃ with concentration (100 ppm) wt% for fuel (D80:B20), compared to diesel fuel, This is due to improvement of the calorific value of fuels. The carbon monoxide decreased for fuel (D80:20:N100 ppm) with changing the air humidity of the intake into the engine of (RH65%) by 62.5%, compared to pure diesel. This is due to increasing the humidification of inlet air which causes the increase of the percentage of oxygen atoms in the cylinder and obtaining a homogeneous concerning fuel, hence more complete combustion occurs [16-18].

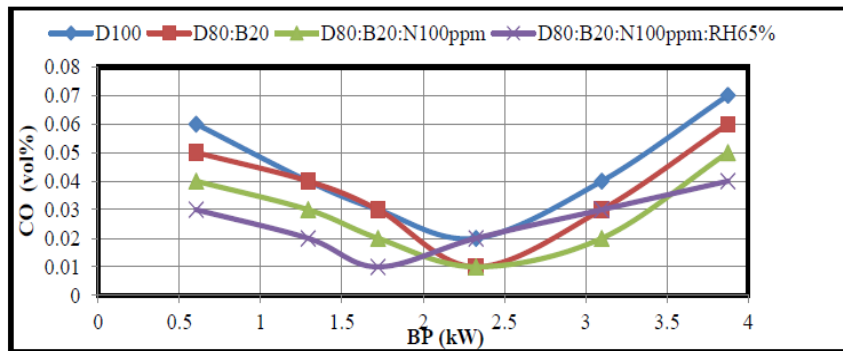


Figure 13: Variation in CO with BP.

2) Unburnt Hydrocarbons Emissions (HC)

Figure 14 exhibits the variation of unburnt hydrocarbons (HC) with the brake power (BP) for all tested fuels (D100, D80:B20, and D80:B20:N100 ppm) with air humidity (RH65%). The unburnt hydrocarbon decreased by 9.76% at the use of fuel (D80:B20), compared to pure diesel, due to the higher oxygen (O₂) concentration in the air-fuel mixture which can help enhance the oxidation of unburnt hydrocarbon. Also, the (HC) decreased by 36% at the addition of nano-Fe₂O₃ with concentration (100 ppm)wt% for fuel (D80:B20), compared to diesel fuel. This is due to improving the calorific value of fuels. The unburnt hydrocarbon decreased by 73.72% for fuel (D80:20:N100 ppm) with changing the air humidity of the intake into the engine of (RH65%), compared to pure diesel. This is due to increasing the humidification of the inlet air which causes the increase of the percentage of oxygen atoms in the cylinder and obtaining a homogeneous concerning fuel, hence more complete combustion occurs [16-18].

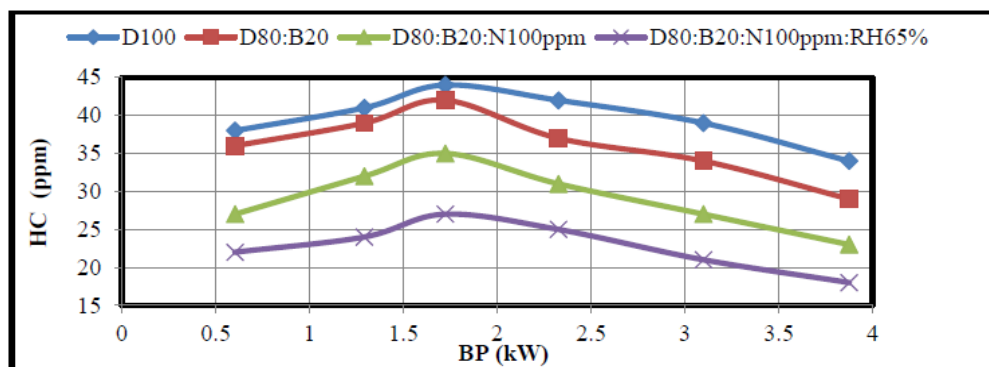


Figure 14: Variation in HC with BP.

3) Nitrogen oxide (NO_x)

Figure 15 illustrates the variation of nitrogen oxide (NO_x) with the brake power (BP) for all tested fuels (D100, D80:B20, and D80:B20:N100 ppm) with air humidity (RH65%). The nitrogen

oxide increased by 8.66% at the use of fuel (D80:B20), compared to pure diesel, due to the higher cetane number of fuel which leads to the higher cylinder temperature. Also, the (NO_x) increased by 16.19% at the addition of nano- Fe_2O_3 with concentration (100 ppm)wt% for fuel (D80:B20), compared to diesel fuel. This is due to higher combustion temperatures caused by added nanoparticles to fuels. But, the nitrogen oxide decreased by 8.45% for fuel (D80:20:N100 ppm) with changing the air humidity of the intake into the engine of (RH65%), compared to pure diesel. This is due to that increasing the humidification of inlet air causes the water droplet to absorb some heat it leads to lower peak temperatures in the combustion zone that reduce the formation rate of NO_x [16,17,18].

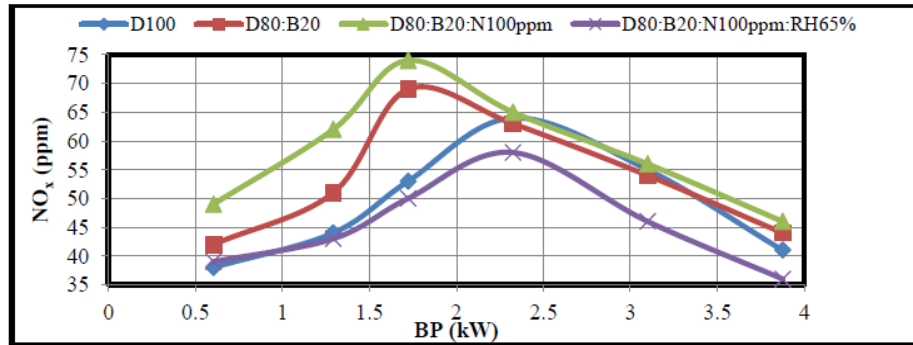


Figure 15: Variation in NO_x with BP.

4) Carbon dioxide emissions (CO_2)

Figure 16 portrays the variation of carbon dioxide (CO_2) with the brake power (BP) for all tested fuels (D100, D80:B20, and D80:B20:N100 ppm) with air humidity (RH65%). The carbon dioxide increased by 13.09% at the use of fuel (D80:B20), due to the higher content oxygen (O_2) concentration in the air-fuel mixture which helps improve the combustion process and the cetane number of fuel which leads to the higher cylinder temperature. Also, the (CO_2) increased by 39.66% at the addition of nano- Fe_2O_3 with concentration (100 ppm)wt% for fuel (D80:B20), compared to diesel fuel. This is due to the enhancement of the physical properties of fuels. Furthermore, the carbon dioxide increased by 45.92% for fuel (D80:20:N100 ppm) with changing the air humidity of intake into the engine of (RH65%), compared to pure diesel. This is due to that increasing the humidification of inlet air causes more consumption of fuel-air mixture, hence higher combustion rate temperature [18].

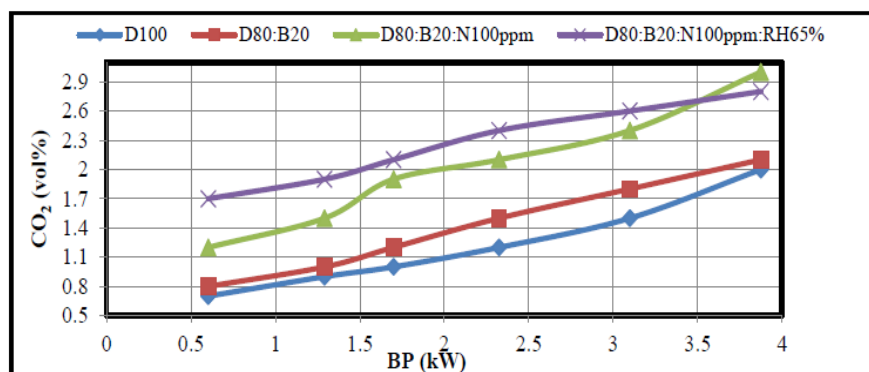


Figure 16: Variation in CO_2 with BP.

5) Smoke Intensity

Figure 17 demonstrates the variation of smoke opacity with the brake power (BP) for all tested fuels (D100, D80:B20, and D80:B20:N100 ppm) with air humidity (RH65%). The smoke opacity decreased by 23.64% at the use of fuel (D80:B20), compared to pure diesel, due to higher thermal efficiency that indicated better and complete combustion of fuel. Also, the smoke opacity decreased by 38.94% at the addition of nano- Fe_2O_3 with concentration (100 ppm)wt% for fuel (D80:B20), compared to diesel fuel. This is due to the improvement of physical properties caused by added nanoparticles to fuels. The smoke opacity decreased by 27.01% for fuel (D80:20:N100 ppm) with

changing the air humidity of intake into the engine of (RH65%), compared to pure diesel. This is due to that increasing the humidification of inlet air causes the longer ignition delay of fuel, where it enables the formation of a homogeneous mixture and thus complete combustion [18].

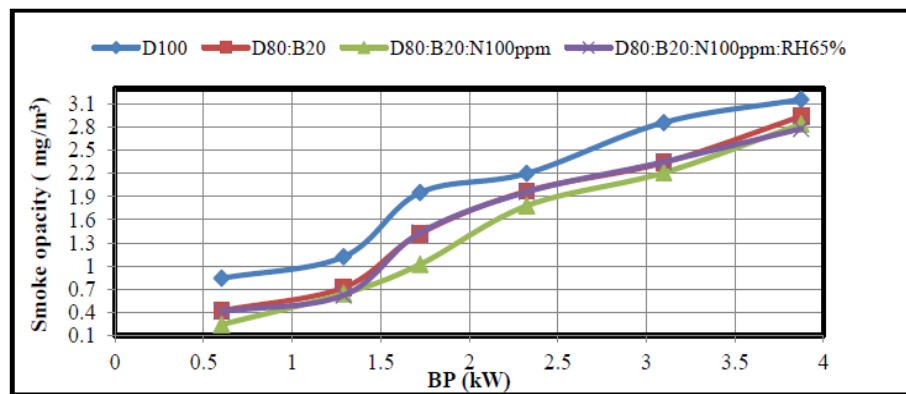


Figure 17: Variation in Smoke opacity with BP.

6) Particulate Matter Emissions (PM)

Figure 18 introduces the variation of particulate matter (PM) with brake power (BP) for all tested fuels (D100, D80:B20, and D80:B20:N100 ppm) with air humidity (RH65%). The particulate matter increased by 12.40% at the use of fuel (D80:B20), compared to pure diesel, due to the higher cetane number of fuel which leads to the higher cylinder temperature. Also, the (PM) increased by 15.30% at the addition of nano-Fe₂O₃ with concentration (100 ppm)wt% for fuel (D80:B20), compared to diesel fuel. This is due to the high combustion temperature caused by added nanoparticles to fuels. However, the particulate matter decreased by 24.17% for fuel (D80:20:N100 ppm) with changing the air humidity of intake into the engine of (RH65%), compared to pure diesel. This is due to that increasing the humidification of inlet air causes the water droplet to absorb some heat, leading to lower peak temperatures in the combustion zone that reduce the formation rate of PM.

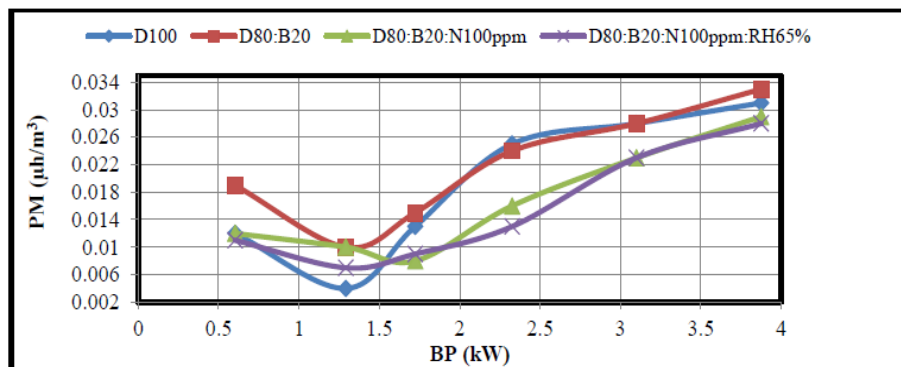


Figure 18: Variation in PM with BP.

4. CONCLUSIONS

This work studied the effects of humidification of air on the performance and exhaust emissions of a single-cylinder four-stroke diesel engine fueled of diesel, biodiesel blended, and nano additives. Also, in this investigation, a water fumigation system was used to change the relative humidity of inlet air over the range (20-65%). The main influences of biofuel, nano additive to the base fuel, and water fumigation are summarized as follows:

- 1) The addition of iron oxide (Fe₂O₃) nanoparticle additive to biofuel (D80:B20) increased the brake thermal efficiency and the brake specific fuel consumption by 15.05%, 11.03%, respectively. Also, the increased air humidity led to improve brake thermal efficiency and brake fuel consumption by 17.62%, 12.72%, respectively.

- 2) The addition of biofuel and nano additive to the base fueled an increase in the NO_x and PM by 16.19%, 15.30%, respectively. While, increasing the humidification of inlet air led to a decrease in the NO_x and PM by 8.45%, 24.17%, respectively.
- 3) Increasing the humidification of the inlet air causes reduced emissions of CO, HC, and smoke opacity by 62.5%, 73.72%, 27.01%, respectively, and CO₂ increased by 45.92%.
- 4) The way of water fumigation into the intake manifold can be used to improve the thermal efficiency and fuel consumption, and also leads to reduce the NO_x and PM emissions.

Nomenclature

WCO	Waste cooking oil
XRD	X- ray Diffraction
SEM	Scanning electron microscope
wt%	Weight ratio
vol%	Volume ratio
VCR	Variable compression ratio
bTDC	Before Top Dead Center
CN	Cetan Number
rpm	Revolution per minute
RH	Relative humidity
ppm	Part per million
DOE	Designing of Experiment
Fe ₂ O ₃	Iron oxide nanoparticle
OA	Orthogonal array
S/N	Signal-to-Noise

Reference

- [1] A. L. Ahmad, N. H. M. Yasin, C. J. C. Derek, J. K. Lim, Microalgae as a sustainable energy source for biodiesel production: a review, *Renew. Sust. Energ. Rev.*, 15 (2011) 584 – 593. <https://doi.org/10.1016/j.rser.2010.09.018>
- [2] C. Carraretto, A. Macor, A. Mirandola, A. Stoppato, S. Tonon, Biodiesel as alternative fuel: experimental analysis and energetic evaluations, *Energy*, 29 (2004) 2195–2211. <https://doi.org/10.1016/j.energy.2004.03.042>
- [3] A. Demirbas, Progress and recent trends in biodiesel fuels, *Energy Convers Manag.*, 50 (2009)14–34. <http://dx.doi.org/10.1016/j.enconman.2008.09.001>
- [4] S. M. Palash, M. A. Kalam, H. H. Masjuki, B. M. Masum, I. M. R. Fattah, M. Mofijur, Impacts of biodiesel combustion on NO_x emissions and their reduction approaches, *Renew. Sustain. Energy. Rev.*, 23 (2013) 473–490. <http://dx.doi.org/10.1016/j.rser.2013.03.003>
- [5] M. Mofijur, A. E. Atabani, H. H. Masjuki, M. A. Kalam, B. M. Masum, A study on the effects of promising edible and non-edible biodiesel feedstocks on engine performance and emissions production: a comparative evaluation, *Renew. Sustain. Energy. Rev.*, 23 (2013) 391–404. <http://dx.doi.org/10.1016/j.rser.2013.03.009>
- [6] M. Mofijur, H. H. Masjuki, M. A. Kalam, A. E. Atabani, M. Shahabuddin, S. M. Palash, M. A. Hazrat, Effect of biodiesel from various feedstocks on combustion characteristics, engine durability and materials compatibility: A review, *Renew. Sustain. Energy. Rev.*, 28 (2013) 441–455. <http://dx.doi.org/10.1016/j.rser.2013.07.051>
- [7] A. K. Affiliation, H. Hernani, R. M. Astuti, R. M. A. Affiliation, A potential study on clove oil, eugenol and eugenyl acetate as diesel fuel bio-additives and their performance on one cylinder engine, *Transp.*, 25 (2010) 66–76. <https://doi.org/10.3846/transport.2010.09>
- [8] T. Shaafi, R. Velraj, Influence of alumina nanoparticles, ethanol and isopropanol blend as additive with diesel–soybean biodiesel blend fuel: combustion, engine performance and emissions, *Renew. Energy.*, 80 (2015) 655–663. <https://doi.org/10.1016/j.renene.2015.02.042>
- [9] A. I. El-Seesy, H. Hassan, S. Ookawara, Effects of graphene nanoplatelet addition to jatropha biodiesel–diesel mixture on the performance and emission characteristics of a diesel engine, *Energy.*, 147 (2018) 1129–1152. <https://doi.org/10.1016/j.energy.2018.01.108>

- [10] J. S. Basha , R.B Anand, An experimental study in a CI engine using nanoadditive blended water–diesel emulsion fuel, *Int. J. Green. Energy.*, 8 (2011) 332– 348. <https://doi.org/10.1080/15435075.2011.557844>
- [11] B. V. A. Rao, M. G. Raju, C. Satyanarayana, Study of performance and exhaust emissions using biodiesel (Mahua Methyl Ester) with water fumigation at the suction end of DI diesel engine, *Pacific Conf. Combust. Center.*, (2007). <http://dx.doi.org/10.13140/RG.2.1.3191.4081>
- [12] T. Belachew, R. Mishra, F. Gu, A. D. Ball, Water injection effects on the performance and emission characteristics of a CI engine operating with biodiesel, *Renew. Energy.*, 37 (2012) 333-344. <http://dx.doi.org/10.1016/j.renene.2011.06.035>
- [13] M. Y. E. Selim, M. T. Ghannam, H. E. Saleh, Behavior of water-waste cooking oil biodiesel emulsion for diesel engine performance, *Int. J. Eng. Res. Technol.*, 9 (2020) 2278-0181. <http://dx.doi.org/10.17577/IJERTV9IS070368>
- [14] A. Parlak, V. Ayhan, İ. Cesur, Investigation of the effects of steam injection on performance and emissions of a diesel engine fuelled with tobacco seed oil methyl ester, *Fuel. Process. Technol.* , 116 (2013) 101–109. <http://dx.doi.org/10.1016/j.fuproc.2013.05.006>
- [15] A. Parlak, A Study on performance and exhaust emissions of the steam injected di diesel engine running with different diesel- conola oil methyl ester blends, *J. Energy. Inst.*, 92 (2019) 717-729. <https://doi.org/10.1016/j.joei.2018.03.001>
- [16] R. Singh, S. Sharma, D. Gangacharyulu, Effect of TiO₂ nanoparticle blended water diesel emulsion fuel on c.i. engine performance and emission characteristics, *Int. J. Eng. Res. Technol.*, 5 (2016) 2278 -0181. <http://dx.doi.org/10.17577/IJERTV5IS070422>
- [17] H. Bandbafha, E. Khalife, M. Tabatabaei, M. Aghbashlo, M. Khanali, P. Mohammadi, T. R. Shojaei, S. Soltanian, Effects of aqueous carbon nanoparticles as a novel nanoadditive in water-emulsified diesel/ biodiesel blends on performance and emissions parameters of a diesel engine, *Energy. Convers. Manag.*, 196 (2019) 1153-1166. <https://doi.org/10.1016/j.enconman.2019.06.077>
- [18] M. Abdollahi, B. Ghobadian, G. Najafi, S. S. Hoseini, M. Mofijur, M. Mazlan, Impact of water–biodiesel–diesel nano-emulsion fuel on performance parameters and diesel engine emission, *Fuel.*, 280 (2020) 118576. <https://doi.org/10.1016/j.fuel.2020.118576>
- [19] J. Ruiz, P. Martínez, N. Martín, Numerical characterization of an ultrasonic mist generator as an evaporative cooler, *Energies.*, 13 (2020) 2971. <https://doi.org/10.3390/en13112971>
- [20] T. M. Patel, N. M. Bhatt, FEM based Taguchi method to reduce the automobile structural member weight, *Gitjet.* 8 (2015) 2–11.